

## Studying the effects of CFRP and GFRP sheets on the strengthening of self-compacting RC girders

Moosa Mazloom<sup>\*1</sup>, Morteza Mehrvand<sup>2</sup>, Pardis Pourhaji<sup>3</sup> and Azim Savaripour<sup>4</sup>

<sup>1</sup>Department of Civil Engineering, Shahid Rajaee Teacher Training University, Tehran, Iran

<sup>2</sup>Department of Civil Engineering, University of Science and Culture, Tehran, Iran

<sup>3</sup>Department of Civil Engineering, Iran University of Science and Technology, Tehran, Iran

<sup>4</sup>Department of Civil Engineering, Islamic Azad University of Sirjan, Sirjan, Iran

(Received February 7, 2019, Revised February 20, 2019, Accepted February 22, 2019)

**Abstract.** One method of retrofitting concrete structures is to use fiber reinforced polymers (FRP). In this research, the shear, torsional and flexural strengthening of self-compacting reinforced concrete (RC) girders are fulfilled with glass fiber reinforced polymer (GFRP) and carbon fiber reinforced polymer (CFRP) materials. At first, for verification, the experimental results were compared with numerical modeling results obtained from ABAQUS software version 6.10. Then the reinforcing sheets were attached to concrete girders in one and two layers. Studying numerical results obtained from ABAQUS software showed that the girders stiffness decreased with the propagations of cracks in them, and then the extra stresses were tolerated by adhesive layers and GFRP and CFRP sheets, which resulted in increasing the bearing capacity of the studied girders. In fact, shear, torsion and bending strengths of the girders increased by reinforcing girders with adding GFRP and CFRP sheets. The samples including two layers of CFRP had the maximum efficiencies that were 90, 76 and 60 percent of improvement in shear, torsion and bending strengths, respectively. It is worth noting that the bearing capacity of concrete girders with adding one layer of CFRP was slightly higher than the ones having two layers of GFRP in all circumstances; therefore, despite the lower initial cost of GFRP, using CFRP can be more economical in some conditions.

**Keywords:** CFRP; GFRP; self-compacting reinforced concrete girder; torsion; bending; shear

### 1. Introduction

Strengthening of concrete structures has been considered recently (Mazloom *et al.* 2018a). In fact, there are novel ways that are worth studying in strengthening of structures (Mazloom *et al.* 2018b). One considerable way of improvement in constructing structures is to use self-compacting concrete (Djebein *et al.* 2018). Self-compacting concrete (SCC) was introduced for the first time in 1986 in Japan, and then this type of concrete was produced in a laboratory in 1988 (Kamura and Ouchi 1998). It showed acceptable results in physical and mechanical features of concrete (Mazloom *et al.* 2018c, Mazloom *et al.* 2018d). In fact, SCC is a kind of concrete that flows under its own weight (Beygi *et al.* 2014). Considering its high level of flowability, it can easily move through the reinforcement, and fill in the molds (Ghasemi 2018). This type of concrete is quite

---

\*Corresponding author, Associate Professor, E-mail: Mazloom@sru.ac.ir; moospoon@yahoo.com

homogeneous, compacted and without any segregation (Afzali Naniz and Mazloom 2018). It is worth noting that using SCC can reduce the cost and time of construction (Nunes *et al.* 2006). Self-compacting concrete (SCC) has been used in many projects due to its high fluidity and the ability to run in reinforced areas (Lin and Lin 2004, Lin and Lin 2005). The use of SCC is appropriate in different parts of structures containing condensed reinforcement (Mazloom *et al.* 2015). In addition, some studies showed that both cohesion and ductility of SCC were more than normal concrete (Chan *et al.* 2003, Paultre *et al.* 2005). In some other cases, stiffness, strength and ductility of SCC were less than normal concrete (Esfahani *et al.* 2008, Chen 2003). Mazloom and Yousefi (2013) predicted the indirect tensile strength of SCC with artificial neural networks.

There are numerous research on reinforcing concrete structures (Mazloom *et al.* 2018a). A lot of research have been done to produce concrete with the appropriate properties (Huang *et al.* 2016, Karamloo *et al.* 2016a, Karamloo *et al.* 2016b). A research presented the development of formulas to estimate the long-term creep and shrinkage of high-strength concrete (Kanema *et al.* 2016). The experimental part of one article concentrated on concrete mixes having water/binder ratio of 0.35 and the total binder content of 500 kg/m<sup>3</sup> (Mazloom2008). In this article, five different percentages of silica fume, which replaced cement were: 0%, 6%, 8%, 10% and 15%. Some equations were proposed for calculating the time-dependent behavior of high-strength concrete due to the experimental results. The accuracy of the recommended equations were verified by several common methods, which were developed for estimating both the creep and the shrinkage of normal strength concrete (Mazloom2008). Also, Mazloom and Ranjbar (2010) studied the relation between the compressive strength of SCC and its workability. They indicated that there was a linear relationship between them in most circumstances.

Some researchers used silica fume in concrete mixes and studied its effects on fresh and hardened properties of concrete (Mazloom and Ramezaniyanpour 2004). Mazloom and Hatami (2015) studied the optimal mix design of self-compacting lightweight concrete (SCLC). They considered the effects of magnetic water, superplasticizer based on polycarboxylic-ether and silica fume on workability of fresh concrete and compressive strength of the hardened one. The results showed that using magnetic water improved compressive strength of all samples at all ages. More superplasticizer was used for the samples that were produced with tap water. In addition, the combination of superplasticizer and magnetic water had positive effects on the mixes having silica fume. Mazloom and Miri (2017) studied the interaction of magnetic water, silica fume and superplasticizer on the fresh and hardened features of concrete. Mazloom *et al.* (2017) studied the effects of a polyepoxide-based superplasticizer and silica fume on fresh and hardened properties of SCLC. They reported the superplasticizer and silica fume improved the durability and mechanical properties of SCLC samples.

In one of the recent studies, the settlement of lightweight coarse aggregate of self-compacting lightweight concrete (SCLC) after placing in its final position is studied (Mazloom and Mahboobi 2017). In this research, the image processing technique of MATLAB software was used to check the segregation. The results showed that the minimum and maximum differences between laboratory tests and software analyses were 1.2% and 9.19% respectively. Mazloom *et al.* (2018c) considered to the effects of rock flour type on both rheology and strength of SCLC too.

Safety is one of the main goals of designing reinforced concrete girders. A sudden failure due to low shear strength is one of its disadvantages. Reinforced concrete beams, at first, should be designed for carrying the bending and shear forces (Al-Nasra and Asha 2013). In some elements of concrete structures, such as edge beams that are connected to slabs, torsional forces can be generated in the elements (Shin and LaFave 2004).

In recent years, the strengthening of structures has increased dramatically (Mardanni-Aghabaglou 2013). In both economic and environmental aspects, rehabilitation and strengthening of the available structures is better than their destruction and reconstruction (Carmona *et al.* 2015). In fact, strengthening is less expensive than reconstruction (Chau-Khun *et al.* 2017). Also, different types of fiber reinforced polymers are used for reinforcing of concrete structures recently (Ashrafi *et al.* 2017, Bazli *et al.* 2019). The behavior of SCC deck slabs reinforced with basalt fiber-reinforced polymer was studied by Zhue *et al.* (2018). Carbon fiber reinforced polymer (CFRP) and glass fiber reinforced polymer (GFRP) have been used for strengthening of different types of structures in structural industry (Saqaan *et al.* 2018, Al-Mahmood *et al.* 2009). An experimental program consisting of 36 direct pull-out tests monitored by acoustic emission were completed to cover the understanding of the bonding behavior of fiber reinforced polymer and steel bars in self-compacting concrete (Di *et al.* 2019). The experimental results proved that the proposed acoustic emission method had enough potential to identify the debonding damage of FRP steel bar reinforced SCC structures accurately.

Banjara and Ramanjaneyulu (2019) studied the flexural deficient RC beams strengthened with CFRP. After confirming load carrying capacities of flexural deficient beams under monotonic loading, they were compared with the performance of control specimens. Hoque and Jumaat (2018) studied a method for predicting debonding failure made by intermediate crack for prestressed FRP in the tension side of the beam. Hamzeh Keykha (2018) presented a numerical study on the behavior of continuous hollow steel beams strengthened with carbon fiber reinforced polymer (CFRP). Eleven samples were analyzed under various coverage lengths, the number of layers, and the location of CFRP composite.

Mastali and Dalvand (2016) present widespread experiments on self-compacting concrete reinforced with recycled CFRP (r-CFRP). They studied the impact of resistance and mechanical properties of the reinforced self-compacting samples. The impact resistance and mechanical properties include both compressive and flexural strength of 252 reinforced cementitious samples with various fiber volume fractions. Analytical analyses were applied to correlate and predict mechanical properties of self-compacting concrete with r-CFRP based on experimental database.

Chellapandian *et al.* (2019) studied the effectiveness of hybrid fiber reinforced polymer strengthening on the total behavioral improvement of reinforced concrete beams under flexure. Eight square RC beams were modeled and strengthened using different FRP techniques including near surface mounting (NSM), external bonding (EB) and hybrid strengthening consuming a combination of NSM carbon FRP laminates and EB CFRP fabric. Experimental results showed that hybrid FRP strengthening could rocket the strength by 160%. In addition, the ultimate displacement of hybrid FRP strengthened beams improved considerably in comparison to NSM technique. Concrete-filled stainless steel tubular (CFSST) columns can be used for bridge piers, multi-story buildings and other supporting structures. The common mode of failure with these types of columns is inelastic external local buckling occurring at the column ends. Sharif *et al.* (2019) presented the results of experimental, numerical and analytical investigations on circular CFSST columns strengthened with carbon fiber reinforced polymer (CFRP) wrap and subjected to axial compression loading.

In this article, numerical models of SCC girders are studied under bending, shear and torsional forces in ABAQUS software version 6.10 to investigate the effects of CFRP and GFRP on the bearing capacity of girder samples. In the first step, numerical models were verified with laboratory tests of Mazloom *et al.* (2015), and then they were strengthened with both glass fiber reinforced polymer (GFRP) and carbon fiber reinforced polymer (CFRP) sheets. Finally, bending,

shear and torsional strengths of all samples were studied to introduce the optimal design of SCC-girders reinforcing with CFRP and GFRP sheets (Fig. 1).

## 2. Verification with ABAQUS software

The ABAQUS software was used for modelling simple girders and reinforced ones with GFRP and CFRP plates and adhesive layers. The finite element analyses were used for these models in the software. At first, plain concrete girders were modelled based on Mazloom *et al.* (2015) for verification. Then concrete girders were reinforced with GFRP and CFRP plates, and the effects of them on shear, torsion and bending were studied. Plain concrete girders were used for torsional models, and reinforced concrete girders were utilized for shear and flexural models. Four tensile bars with the diameter 20 mm were intended for the modelling of shear girders. Two bars with the diameter 20 mm were used in the above of flexural girders. In addition, all of them had stirrups with the diameter of 12 mm. The distance between the stirrups were the same and equal to 100 mm.

## 3. Sample features

The dimensions of samples are the same and equal to 300\*300 mm<sup>2</sup>. Fig. 2 shows the properties of models to calculate flexural stresses. The girders were loaded according to four points bending test method. The properties of concrete beams, steel, GFRP, CFRP and adhesive layer are presented in Tables 1 to 5.

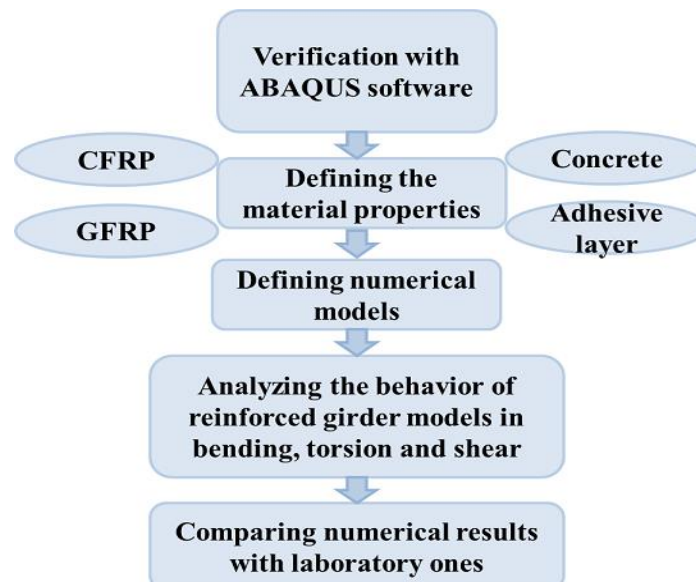


Fig. 1 A detailed flowchart of the research

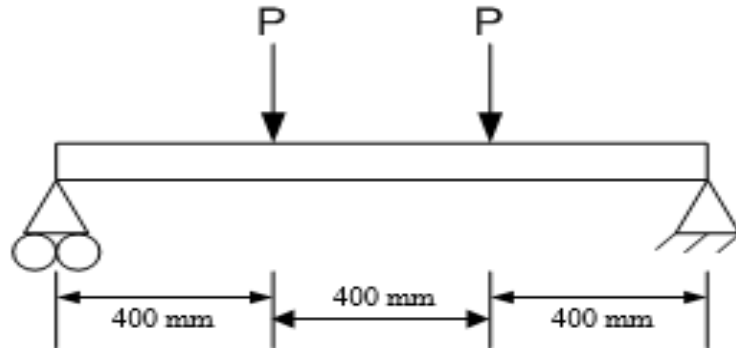


Fig. 2 The setup test for calculating the flexural stresses

The behaviours of reinforced beams in bending and shear were studied under four point loads with finite element method and nonlinear analysis. In torsion models, the loads were applied outside the symmetry axis and at the two ends of concrete girders (Mazloom *et al.* 2015).

Table 1 Features of concrete girder

Girder	Dimensions (mm)			Tensile strength (MPa) = $f_t'$	Compressive strength (MPa) = $f_c'$	Elastic modulus (MPa) = $E_c$	FRP	
	B	H	L				Sheet thickness	Number of layers
B1	300	300	1200	3.17	30	24870	0	0
B2	300	300	1200	3.17	30	24870	0.165	1
B3	300	300	1200	3.17	30	24870	0.33	2

Table 2 The specifications of GFRP sheets

Ultimate tensile strength (MPa)	Modulus of Elasticity (GPa)	Rupture strain (%)
3400	72.413	4.5

Table 3 The qualifications of CFRP sheets

Ultimate tensile strength (MPa)	Modulus of Elasticity (GPa)	Rupture strain (%)
3450	235	1.5

Table 4 The specifications of steel bars

Poisson's Ratio	Elastic modulus (GPa)	$f_u$ (MPa)	$f_y$ (MPa)
0.2	200	600	400

Table 5 The characteristics of adhesive layers

Elastic modulus (MPa)	G (MPa)	Thickness (mm)
1824	622	0.636

### 3.1.1 Main concrete specifications

Concrete is a kind of material with complex behaviours. It also has a nonlinear behaviour in high levels of stresses. For simulating concrete behaviours, the models that consider the damage effects and plasticity are more appropriate (Hansen *et al.* 2001). In this research, a damaged concrete model or a CDP model is used for concrete modelling. In this model, two rupture mechanisms for concrete, which are tensile cracking and compression crushing, are assumed. Both of these phenomena are due to the beginning and expansion of the cracks. The stress-strain behaviour of concrete should be defined under uniaxial pressure. It is supposed that the behaviour of uniaxial tensile stress of concrete is linear until the formation of finite cracks when the maximum stress becomes equal to tensile strength.

The behaviour of concrete after failure should be determined in terms of fracture strain. This method considers the interaction effects between concrete and reinforcement. In addition, the effects of the distribution of concrete stresses after cracking should be entered into the calculations (Tajieddin 2008). ABAQUS theory was used for defining plastic behaviour of concrete in CDP models (ABAQUS 2010).

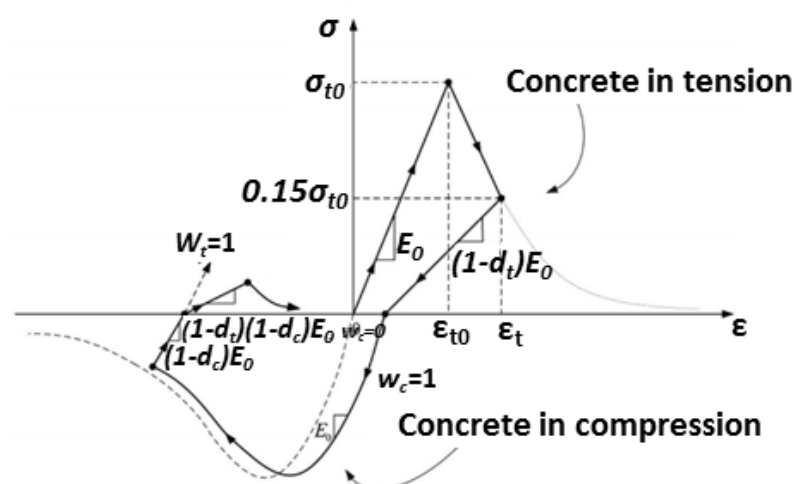


Fig. 3 Concrete behavior curve in compression and tension under axial compressive loading

3.1.2 Stress-strain behavior of concrete

As shown in Figs. 3 and 4, equivalent plastic strain can be calculated with the compressive stress and strain of the concrete, failure parameters and the elasticity modulus of the concrete. Based on Figs. 5 and 6, the simplified relations were used to calculate the compressive stress-strain curves in this research (Hogenstad 1951).

When the cracks in a reinforced concrete element appear, it can still withstand tensile stresses in the perpendicular direction of the cracks, which is called the residual tensile strength (Fig. 7). In this research, a strain method was used to introduce concrete tensile behavior to the software. Table 6 shows the stress and strain of concrete cracks and their failure parameters.

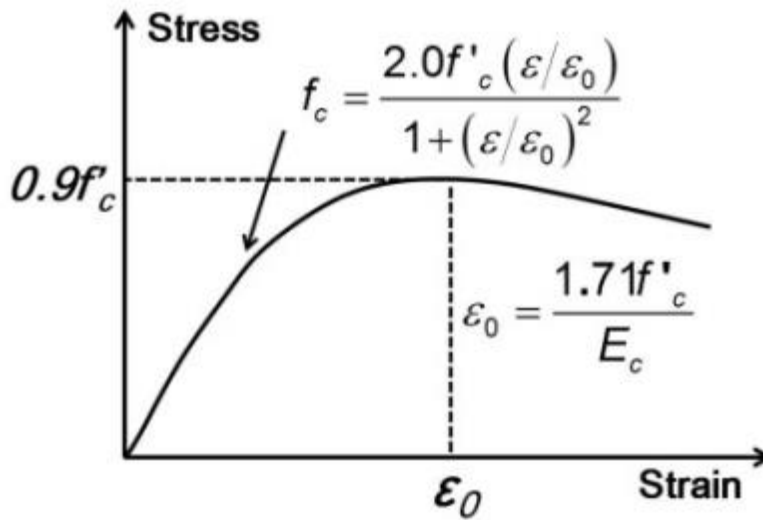


Fig. 4 Concrete behavior in compression under axial compressive loading

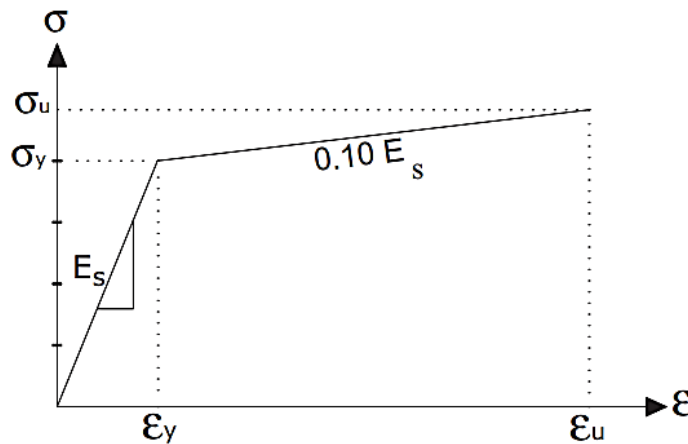


Fig. 5 Steel stress-strain curve

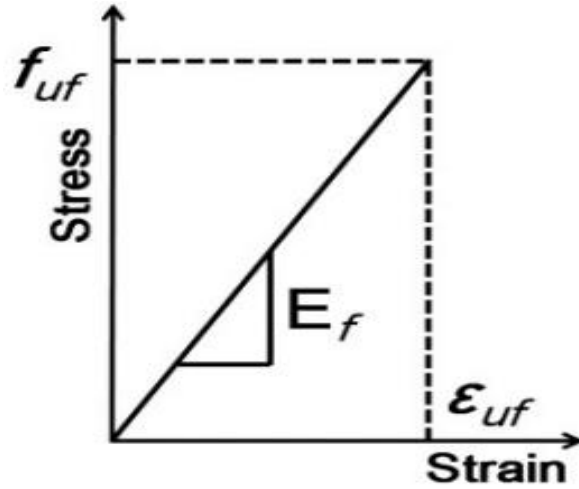


Fig. 6 FRP stress-strain curve

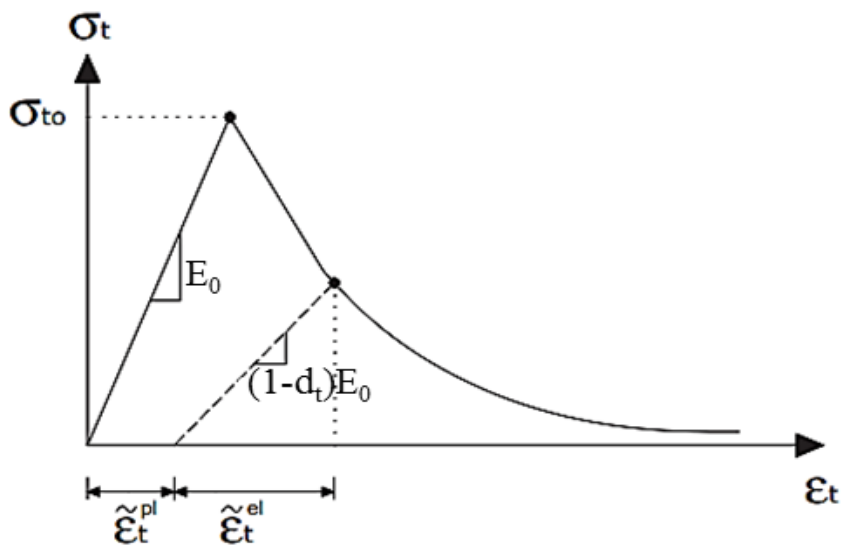


Fig. 7 Concrete behavior curve in tension

Table 6 Properties of stress and strain concrete cracks in tension and its failure parameter

Tensile stress	Tensile strain	Failure parameter
3.17	0	0
0	0.00128	0.9

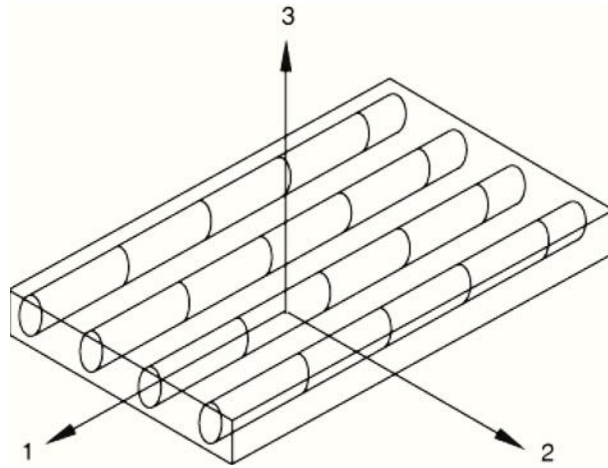


Fig. 8 Single-sided sheet

### 3.2 Fiber reinforced polymer

Fiber Reinforced polymers (FRP) have linear stress-strain behaviors. In fact, FRP materials have elastic and linear behaviors up to the point of failure (reaching to the final strain,  $\varepsilon_u$ ); then crispy fracture occurs in their final strength (Fig. 6). Kok (2004) suggests using elastic linear behavior for FRP materials.

As shown in Fig. 8, the carbon fibers in FRP materials are assumed to be parallel. For this model, the properties of materials should be defined in the local coordinate system by the user. The plate was on the surface 1-2 and the local direction one, which was related to the direction of fiber. The response of the damaged material should be defined as well.

### 3.3 Adhesive layer

The investigation of early destruction resulting from the separation depends on adding the interface model to the general model. In this study, this was done by modeling the adhesive layer and defining the properties and mechanical behavior of this layer. The adhesive behavior was defined as a traction-separation model in the software. This model had two modes: the loss of adhesion and the elastic fracture in tensile stress. The relative displacement was caused by the slip ( $\delta$ ) in the adhesive layer. In this model, the final value of the relative displacement ( $\delta_f$ ) and the initial crack value ( $\delta_0$ ) depended on following input parameters (Eq. (1)).

$$k_0 = \frac{\tau_{\max}}{\delta_0}, \quad \delta_f = \frac{2G_{cr}}{\tau_{\max}} \quad (1)$$

The behavior of adhesive layer was modeled with defining the elastic and destructed modes of the glue. The initial behavior of adhesive layer was in form of the elastic-linear behavior at the beginning of failure, and it should be defined with the initial stiffness vector (Eq. (2)):

$$K_m = \frac{E}{t}, \quad K_{tr} = \frac{G_1}{t}, \quad K_{ss} = \frac{G_2}{t} \quad (2)$$

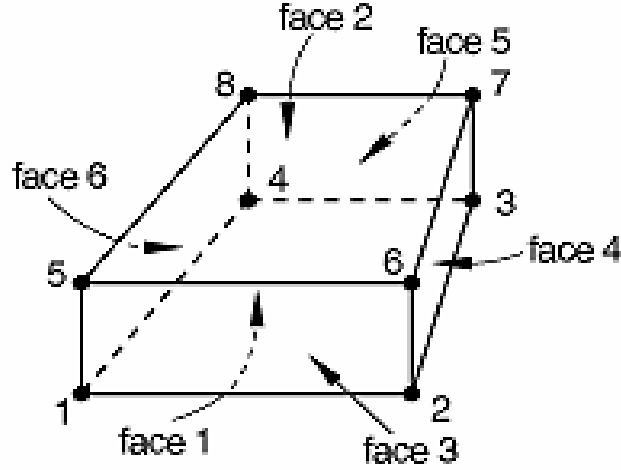


Fig. 9 Eight-node three dimensional cohesive element (COH3D8)

In this equation,  $t$  is the adhesive thickness,  $E$  is the adhesive elastic modulus,  $G_1$  and  $G_2$  are the shear modulus of adhesive in the second and third directions of the plate,  $K_m$ ,  $K_{tt}$  and  $K_{SS}$  are the initial stiffness in the perpendicular directions and two other main directions according to Fig. 9. Defining the failure fraction to the software included the behavior of failure in the beginning and its spreading. In the adhesive failure hypothesis, the failure starts when the second-order strain equation including the principal stress ratios equals to one (Eq. (3)).

$$\left\{ \frac{\sigma_n}{\sigma_n} \right\}^2 + \left\{ \frac{\tau_n}{\tau_n} \right\}^2 + \left\{ \frac{\tau_t}{\tau_n} \right\}^2 = 1 \quad (3)$$

The  $\sigma_n$ ,  $\sigma_t$  and  $\sigma_s$  parameters are the maximum tensile and shear stresses of adhesive layer, and  $n$ ,  $s$  and  $t$  are the stress components in elastic range (Fig. 10).

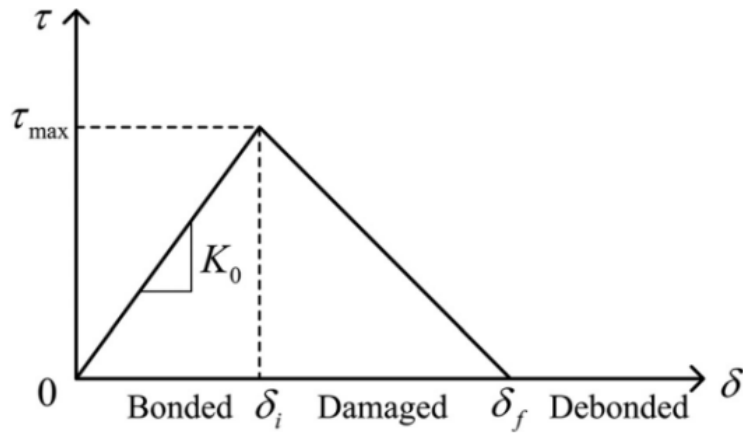


Fig. 10 Adhesive layer behavior

The values of these parameters were proposed as:  $\sigma_s = \sigma_t = \tau_{max}$  and  $\sigma_n = f_{ct}$ . The  $f_{ct}$  is the maximum tensile stress and  $\tau_{max}$  is the maximum shear stress of concrete which can be obtained from Eqs. (4) and (5)

$$\tau_{max} = 1.5\beta_w f_{ct} \quad (4)$$

$$\beta_w = \sqrt{\frac{(2.25 - \frac{b_f}{b_c})}{(1.25 + \frac{b_f}{b_c})}} = 0.75 \quad (5)$$

The value of  $b_f/b_c$  in the reinforced beam was equal to 1;  $b_f$  is the width of FRP plate,  $b_c$  is the concrete width and  $f_{ct}$  is the tensile strength of concrete. Numerical simulations showed that this value was very high for the maximum shear stress; so  $\tau_{max}/2$  was replaced with it (Eqs. (6) and (7)).

$$\tau_s^0 = \tau_t^0 = \frac{\tau_{max}}{2} = 1.78 \text{ MPa} \quad (6)$$

$$\sigma_n^0 = f_{ct} = 3.1 \text{ MP} \quad (7)$$

The hypothesis of the expansion of adhesive failure is expressed in terms of released energy. In ABAQUS software, the dependence of the failure energy was defined on the basis of the BK rupture criterion as follows (Eq. (8))

$$G_n^c + (G_s^c - G_n^c) \left\{ \frac{G_\phi}{G_\psi} \right\}^\eta = G^c \quad (8)$$

The material parameters are  $G_\psi = G_n + G_s$ ,  $G_\phi = G_s + G_t$  and  $\eta$ . The values  $G_n$ ,  $G_s$  and  $G_t$  are related to the work, which is done by strain. This criterion is valuable especially when the critical failure energies are the same during the total deformation in the first and second directions of stresses ( $G_s^c = G_t^c$ ). The values used in this research are:  $G_n^c = 111.52 \text{ J/m}^2$ ,  $G_s^c = G_t^c = 900 \text{ J/m}^2$ , and  $\eta = 1.45$ . In addition, the value of  $G_n^c$  is calculated with the experimental relations of the failure energy. It is equal to the underneath area of the concrete's softening curve (Lu *et al.* 2005).

$$G_F = 2.5\alpha_0 \left( \frac{f_c'}{0.051} \right)^{0.46} \left( 1 + \frac{d_a}{11.27} \right)^{0.22} \left( \frac{w}{c} \right)^{-0.3} \quad (9)$$

The concrete softening curve was intended under single axial tensile load in this study. The tensile strength of concrete that controls the starting point of fine cracks in concrete is  $f_t'$ , and  $G_f$  is the total fracture energy that needs to start, expand, and break a complete crack per unit area. In Eq. (9), the compressive strength of concrete is  $f_c'$  (MPa), and concrete fracture energy is  $G_f$  (N/m).

#### 4. Elements used in numerical analysis

In concrete modeling due to its three-dimensional behavior, C3D8R was used to model concrete, and T3D2 were used for tensile and compressive steel respectively. In addition, the S4R element shell, which is a 4-node element was used for GFRP and CFRP plates. The COH3D8 element was intended for the adhesive plate. A Hex-shaped meshing was used for GFRP and CFRP sheets in the modeling of concrete girder and adhesive layer elements. Figs. 11-13 show the numerical models for bending, shear and torsion loadings. The GFRP and CFRP plates were used to reinforce bending girders at the bottom of them. The GFRP and CFRP, which were twisted around the concrete girder, were used to reinforce the beam against torsion.

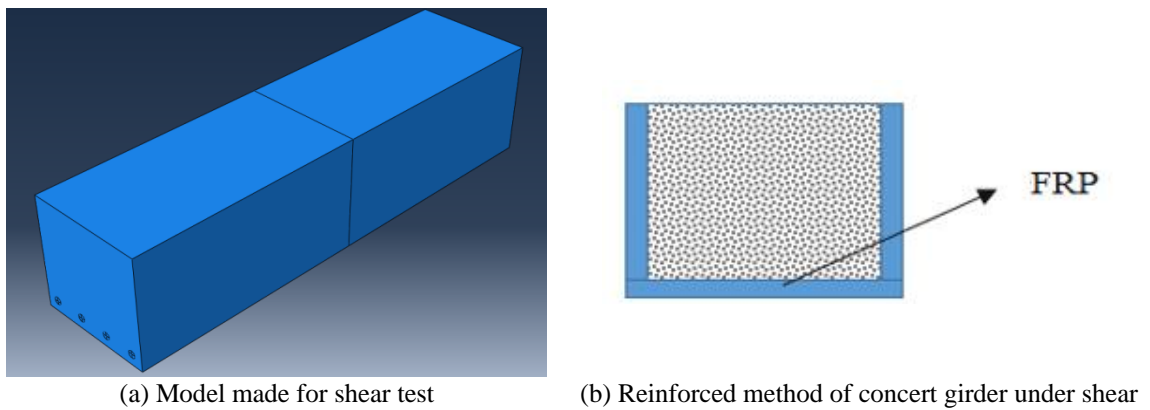


Fig. 11 Detail of the model used in shear test

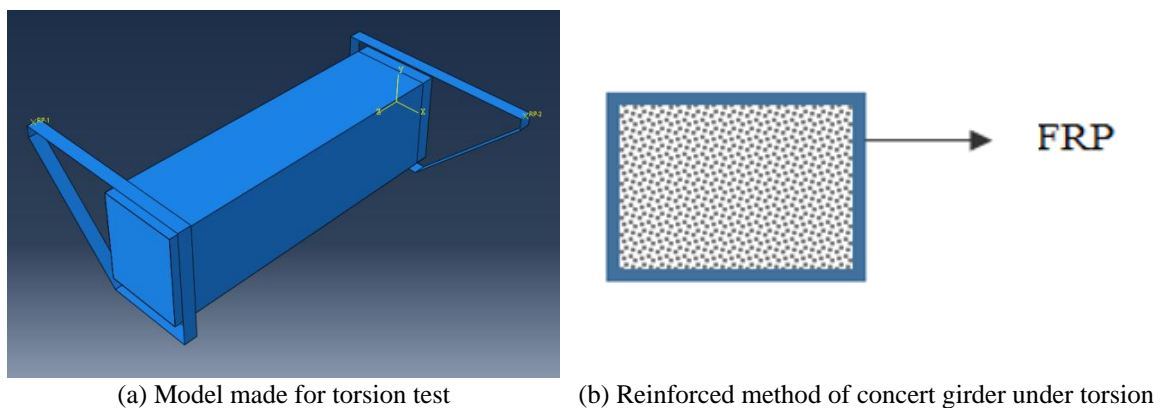


Fig. 12 Detail of the model used in torsion test

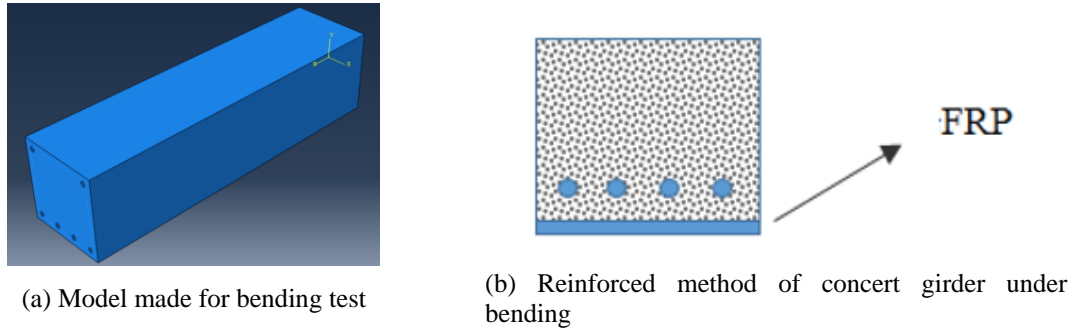


Fig. 13 Detail of the model used in bending test

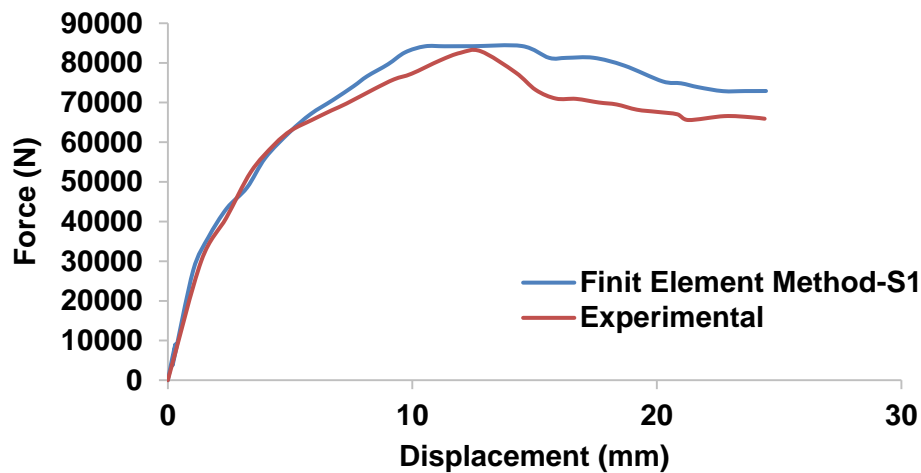


Fig. 14 Force-displacement curve for simple girder under loading for calculating shear

## 5. Results of numerical models

In the first step, the numerical results are obtained from shear models, and then the results of the torsional and bending models are expressed. The relation between force and displacement is nonlinear for nonlinear analysis, and the stiffness of the structure is the displacement function. To solve such equations, the load cannot be applied to the structure at once, and the problem can be solved by dividing the applied load into the small steps. In fact, the condition of convergence in the results happens during gradual loading. In this research, the Newton-Raphson method was used to achieve convergence.

### 5.1 Shear results

Load-displacement curves for control beams are shown in Fig. 14, and both GFRP and CFRP reinforced girders are exhibited in Fig. 15 with the software. In these figures, the values of lateral and vertical displacements are plotted in the middle of the girders. The results of the beam models

in the software (numerical modeling) are almost the same as the laboratory results, and the error rate between the numerical models and the laboratory tests are negligible. In fact, the numerical and laboratory results are very well matched in the elastic region.

The numerical values obtained from modeling are presented in Table 7. In this table, various types of studied girders, the method of strengthening and the thickness of the layers of GFRP and CFRP, the maximum load of the laboratory samples and the maximum numerical load of the models are shown. The differences between the numerical and laboratory results were less than 2%. In reinforcing concrete girders against shear, the bearing capacity of girders improved up to 32% with adding one layer of reinforced GFRP sheet, and it increased up to 45% with adding two layers of reinforcement sheets. Therefore, the performance of double layers of GFRP was proper for shear strengthening. In reinforcing of concrete girders against shear, the bearing capacity increased up to 55% by adding one layer of CFRP sheet, and increased up to 90% by adding two layers of it.

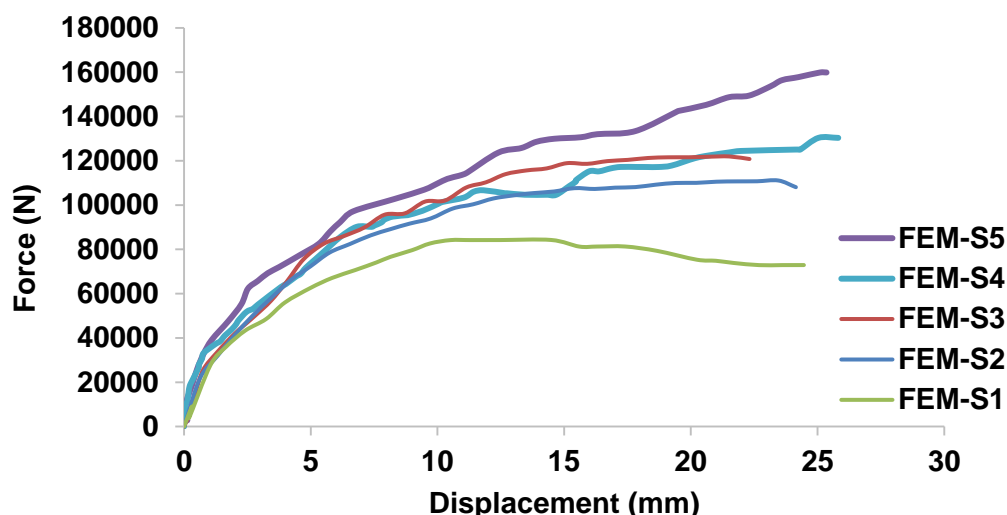


Fig. 15 Force-displacement curve for reinforced girders under loading for calculating shear

Table 7 Numerical characteristics obtained from models under loading for calculating shear

Girder	Reinforcing type	Thickness (mm)	Maximum laboratory load (N) [17]	Maximum numerical model load (N)	Increased reinforced girder capacity (%)
S1	---	0	82953.16	84241.44	---
S2	1 layer of GFRP	0.165	82953.16	111089.90	32
S3	2 layers of GFRP	0.33	82953.16	121950.35	45
S4	1 layer of CFRP	0.165	82953.16	130351.75	55
S5	2 layers of CFRP	0.33	82953.16	159860.83	90

### 5.2 Torsion results

The load-rotation curves are shown in Fig. 16 for the control girders; the software results of GFRP and CFRP reinforced beams are shown in Fig. 17. The rotation values were plotted in the two ends of beams. The accuracy of models was very respectable and the error rate between the software and laboratory results were less than 10%. Actually, both numerical and laboratory results were very well matched in the elastic and plastic areas.

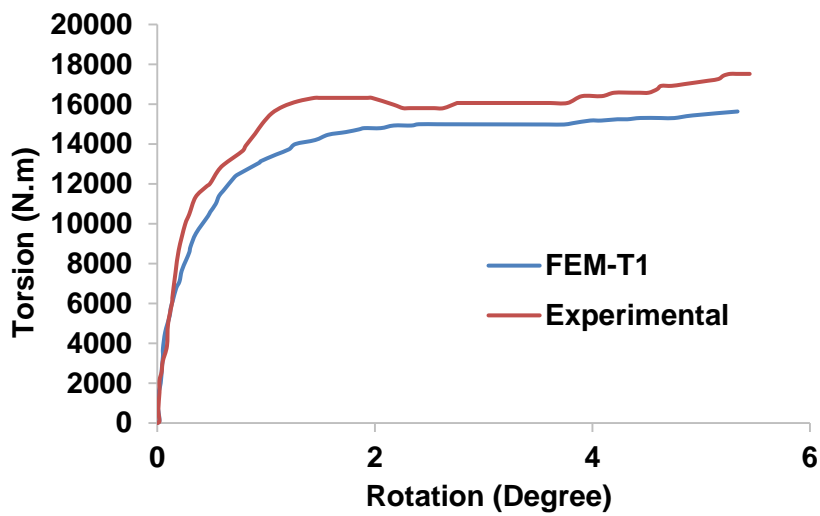


Fig. 16 Force-displacement curve for simple girder under loading for calculating torsion

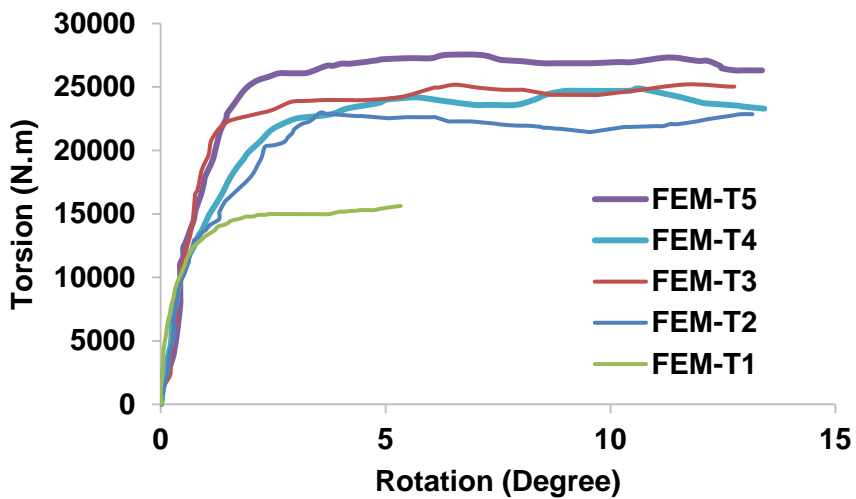


Fig. 17 Force-displacement curve for reinforced girders under loading for calculating torsion

Table 8 Numerical characteristics obtained from models under loading for calculating torsion

Girder	Reinforcing type	Thickness (mm)	Maximum laboratory load (N) [17]	Maximum numerical model load (N)	Increased reinforced girder capacity (%)
T1	---	0	17518.01	15631.34	---
T2	1 layer of GFRP	0.165	17518.01	22965.53	47
T3	2 layers of GFRP	0.33	17518.01	25199.10	61
T4	1 layer of CFRP	0.165	17518.01	24868.53	59
T5	2 layers of CFRP	0.33	17518.01	27528.73	76

The numerical values obtained from modeling are presented in Table 8. In this table, different types of studied beams, strengthening and thickness of GFRP and CFRP layers, the maximum load of laboratory sample and the maximum numerical load of modeling are shown. The error resulting from the numerical and laboratory models were less than 11%. The torsional load capacity improved about 47% by adding one layer of GFRP sheet and enhanced 61% by adding two layers of it. Under torsion loading, the bearing capacity of girders increased about 59% by adding one layer of CFRP sheet, and it increased up to 76% by adding two layers of CFRP sheet.

### 5.3 Bending results

The concrete beams were modeled for further study on bending and were examined under 4-point loading. In this section, the numerical results of finite element method were obtained from the software. Then, the effects of strengthening with GFRP and CFRP plates were studied in the models. Fig. 18 shows Load-displacement curves for beams without reinforcing, GFRP reinforced beams and CFRP ones. The values of vertical displacement in the middle of beams are plotted in this figure.

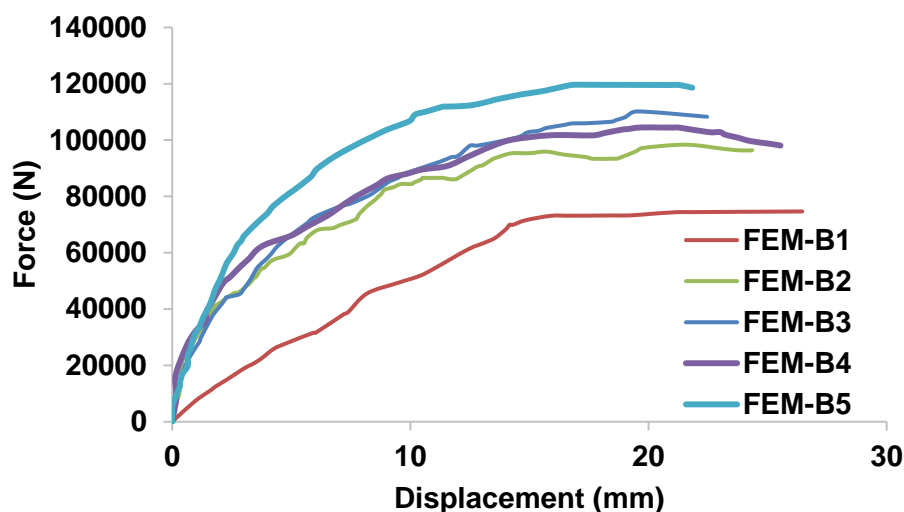


Fig. 18 Force-displacement curves of girder samples for calculating bending

Table 9 Numerical characteristics obtained from models under loading for calculating bending

Girder	Reinforcing type	Thickness (mm)	Maximum numerical model load (N)	Increased reinforced girder capacity (%)
B1	---	0	74652.40	---
B2	1 layer of GFRP	0.165	98351.76	32
B3	2 layers of GFRP	0.33	110175.31	48
B4	1 layer of CFRP	0.165	104468.35	40
B5	2 layers of CFRP	0.33	119643.35	60

The numerical values, which were obtained from modeling, are presented in Table 9. This table shows numerous types of studied beams, method of strengthening and thickness of GFRP and CFRP layers, maximum load of laboratory sample and maximum load of numerical modeling. Strengthening results for bending of concrete girders were roughly the same as those obtained for shear. Bearing capacity increased about 32% by adding one layer of GFRP under the girder, and it increased up to 48% with the addition of two layers of this reinforcement sheet. In fact, the performance of double layers of GFRP had quite satisfactory results for flexural strengthening. The flexural bearing capacity of concrete girders increased up to 40% by adding one layer of CFRP sheet under the girders, and it increased up to 60% by adding two layers of this reinforcement sheet.

To sum up, the results of the strengthening of concrete girders including CFRP showed that the load bearing capacity of these samples in torsion, bending and shear were greater than the samples having GFRP with the same number of layers. In fact, the bearing capacity of concrete girders with adding one layer of CFRP were almost the same as the ones having two layers of GFRP in all circumstances. Although the initial cost of GFRP is lower than CFRP, using the latter one can be more economical in some conditions. Moreover, there are various research in reinforcing beams with CFRP and GFRP; they have explained CFRP was better than GFRP in different tests while GFRP beams had their own positive features (Attari *et al.* 2012, Silva *et al.* 2013).

## 6. Conclusions

Based on the analysis of the test results, the following conclusions can be presented:

- The results of the strengthening of concrete girders including CFRP showed that the load bearing capacity of these samples in torsion, bending and shear were higher than the samples having GFRP with the same number of layers. In fact, the bearing capacity of concrete girders with adding one layer of CFRP were almost the same as the ones having two layers of GFRP in all circumstances.
- In reinforcing concrete girders against shear, the bearing capacity of girders increased up to 32% with adding one layer of GFRP sheet, and it rocketed up to 45% with adding two layers of reinforcement sheets. Therefore, the performance of double layers of GFRP was proper for shear strengthening. In reinforcing of concrete girders against shear, the bearing capacity increased up to 55% by adding one layer of CFRP sheet, and increased up to 90% by adding two layers of it.

- The torsional load capacity increased about 47% by adding one layer of GFRP sheet and enhanced 61% by adding two layers of it. Under torsional loading, the bearing capacity of girders increased about 59% by adding one layer of CFRP sheet, and it increased up to 76% by adding two layers of CFRP sheet.
- Strengthening results for bending of concrete girders were roughly the same as those obtained for shear. Bearing capacity increased about 32% by adding one layer of GFRP under the girder, and it increased up to 48% with the addition of two layers of this reinforcement sheet. In fact, the performance of double layers of GFRP had quite satisfactory results for flexural strengthening. The flexural bearing capacity of concrete girders increased up to 40% by adding one layer of CFRP sheet under the girders, and it increased up to 60% by adding two layers of this reinforcement sheet.

## References

- ABAQUSE (2010), Abaqus theory manual and user manual and Example Manual Version 6.10. Providence.
- ACI Committee 209 (2008), Prediction of Creep, Shrinkage and Temperature Effects in Concrete Structures, Designing for Creep and Shrinkage in Concrete Structures, SP-76, *American Concrete Institute*, Farmington Hills, USA.
- Afzali Naniz, O. and Mazloom, M. (2018), "Effects of colloidal nano-silica on fresh and hardened properties of self-compacting lightweight concrete", *J. Build. Eng.*, **20**, 400-410.
- Al-Mahmoud, F., Castel, A., François, R. and Tourneur, C. (2009), "Strengthening of RC members with near-surface mounted GFRP rods", *Compos. Struct.*, **91**(2), 138-147.
- Al-Nasra, M.M. and Asha, N.M. (2013), "Shear reinforcements in the reinforced concrete beams", *Am. J. Eng. Res. (AJER)*, **2**(10), 2320-0847.
- Ashrafi, H., Bazli, M., Pournamazian Nazafabadi, E. and Vatani Oskouei, A. (2017), "The effect of mechanical and thermal properties of FRP bars on their tensile performance under elevated temperatures", *Constr. Build. Mater.*, **157**, 1001-1010.
- Attari, N., Amziane, S. and Chemrouk, M. (2012), "Flexural strengthening of concrete beams using CFRP, GFRP and hybrid FRP sheets", *Constr. Build. Mater.*, **37**, 746-757.
- Banjara, N. and Ramanjaneyulu, K. (2019), "Effective CFRP retrofit strategy for flexural deficient RC beams", *Struct. Eng. Mech.*, **69** (2), 163-175.
- Bazli, M., Ashrafi, H., Jafari, A., Zhao, X., Gholipour, H. and Vatani Oskouei, A. (2019), "Effect of thickness and reinforcement configuration on flexural and impact behavior of GFRP laminates after exposure to evaluated temperatures", *Compos. Part B: Eng.*, **157**, 76-99.
- Beygi, M.H.A., Kazemi, M.T., Nikbin, I.M., Vaseghi Amiri, J., Rabbanifar, S. and Rahmani, E. (2014), "The influence of coarse aggregate size and volume on the fracture behavior and brittleness of self-compacting concrete", *Cement Concrete Res.*, **66**, 75-90.
- Carmona, J., Garces, P. and Climent, M.A. (2015), "Efficiency of a conductive cement-based anodic system for the application of cathodic protection, cathodic prevention and electrochemical chloride extraction to control corrosion in reinforced concrete structures", *Corrosion Science*, **96**, 102-111.
- Chan, Y.W., Chen, Y.S. and Liu, Y.S. (2003), "Development of bond strength of reinforcement steel in self-consolidating concrete", *ACI Struct. J.*, **100**(4), 490-498.
- Chellapandian, M., Suriya Prakash, S. and Sharma, A. (2019), "Experimental and finite element studies on the flexural behavior of reinforced concrete elements strengthened with hybrid FRP technique", *Compos. Struct.*, **208**, 466-478.
- Chen, Y.F. (2003), "An investigation on confinement behavior of square self-compacting concrete columns", Master dissertation, National Taiwan University, Taiwan.

- Di, B., Wang, J., Li, H., Zheng, J., Zheng, Y. and Song, G. (2019), "Investigation of bonding behavior of FRP and steel bars in self-compacting concrete structures using acoustic emission method", *Sensors*, **19**(1), 159-173.
- Djebien, R., Hebhouh, H., Belachia, M., Berdoudi, S. and Kherraf, L. (2018), "Incorporation of marble waste as sand in formation of self-compacting concrete", *Struct. Eng. Mech.*, **67** (1), 87-91.
- Esfahani, M. R., Lachemi M. and Kianoush M. R. (2008), "Top-bar effect of steel bars in self-consolidating concrete (SCC)", *Eng. Struct.*, **30**, 52-60.
- Ghasemi, M., Ghasemi, M.R. and Mousavi, S.R. (2018), "Investigating the effects of maximum aggregate size on self-compacting steel fiber reinforced concrete fracture parameters", *Constr. Build. Mater.*, **162**, 674-682.
- Hamzeh Keykha, A. (2018), "Numerical investigation of continuous hollow steel beam strengthened using CFRP", *Struct. Eng. Mech.*, **66**(4), 439-444.
- Hansen, E., Willam, K. and Carol, I. (2001), "A two surface anisotropic damage/plasticity model for plain concrete", *Proceedings of the Francos-4 Conference Paris*, Rotterdam, May.
- Hogenstad, E. (1951), "A Study Of Combined Bending And Axial Load In Reinforced Concrete Members", Urbana, Ill. University of Illinois 1951, Urbana, Illinois, USA.
- Hoque, N. and Jumaat, M. (2018), "Debonding failure analysis of prestressed FRP strengthened RC beams", *Struct. Eng. Mech.*, **66** (4), 543-555.
- Huang, H., Qian, C., Zhao, F., Qu, J., Guo, J. and Danzinger, M. (2016), "Improvement on microstructure of concrete by polycarboxylate superplasticizer (PCE) and its influence on durability of concrete", *Constr. Build. Mater.*, **110**, 293-299.
- kamura, H. and Ouchi, M (1998), "Self- compacting high performance concrete", *Concrete Int.*, **1**(4), 378-383.
- Kanema, J.M., Eid, J. and Taibi, S. (2016), "Shrinkage of earth concrete amended with recycled aggregates and superplasticizer: Impact on mechanical properties and cracks", *Mater. Des.*, **109**, 378-389.
- Karamloo, M., Mazloom, M. and Payganeh, G. (2016a), "Effects of maximum aggregate size on fracture behaviors of self-compacting lightweight concrete", *Constr. Build. Mater.*, **123**, 508-515.
- Karamloo, M., Mazloom, M. and Payganeh, G. (2016b), "Influences of water to cement ratio on brittleness and fracture parameters of self-compacting lightweight concrete", *Eng. Fract. Mech.*, **168**, 227-241.
- Kok, L. (2004), "Effect of beam size and FRP thickness on interfacial shear stress concentration failure mode in FRP strengthened beam", Master Dissertation, National University of Singapore, Singapore.
- Lin, C. H. and Lin, S.P. (2005), "Flexural behavior of high-workability concrete columns under cyclic loading", *ACI Structural Journal*, **102**(3), 412-421.
- Lin, C. H., Lin, S.P. and Tseng, C. H. (2004), "High workability concrete columns under concentric compression", *ACI Struct. J.*, **101**(1), 85-93.
- Lu, X.Z., Ten, J.G., Ye, L.P. and Jaing, J.J. (2005), "Bond-slip models for FRP sheets/plates bonded to concrete", *Eng. Struct.*, **24**(5), 920-37.
- Ma, C., Apandi, N.M., Yung, S.C.S., Hau, N., Haur, L.W., Zawawi Awang, A. and Omar W. (2017), "Repair and rehabilitation of concrete structures using confinement: A review", *Constr. Build. Mater.*, **133**, 502-515.
- Mardani Aghabaglou, A., Tuyan, M., Yılmaz, G., Arıöz, Ö. and Ramyar, K. (2013), "Effect of different types of superplasticizer on fresh, rheological and strength properties of self-consolidating concrete", *Constr. Build. Mater.*, **47**, 1020-1025.
- Mastali, M. and Dalvand, A. (2016), "The impact resistance and mechanical properties of self-compacting concrete reinforced with recycled CFRP pieces", *Compos. Part B: Eng.*, **92**, 360-376.
- Mazloom, M. (2008), "Estimating long-term creep and shrinkage of high-strength concrete", *Cement Concrete Compos.*, **30**(4), 316-326.
- Mazloom, M., Afkar, H. and Pourhaji, P. (2018b), "Assessing the ductility of moment frames utilizing genetic algorithm and artificial neural networks", *Struct. Monit. Maint.*, **5** (4), 445-461.
- Mazloom, M., Allahabadi, A. and Karamloo, M. (2017), "Effect of silica fume and polyepoxide-based polymer on electrical resistivity, mechanical properties, and ultrasonic response of SCLC", *Adv. Concrete*

- Constr.*, **5**(6), 587-611.
- Mazloom, M. and Hatami, H. (2015), "The behavior of self-compacting light weight concrete produced by magnetic water", *Int. J. Civil, Environ. Struct. Constr. Architect. Eng.*, **9**(12), 1616-1620.
- Mazloom, M., Homayooni, S.M. and Miri, S.M. (2018c), "Effect of rock flour type on rheology and strength of self-compacting lightweight concrete", *Comput. Concrete*, **21**(2), 199-207.
- Mazloom, M. and Mahboobi, F. (2017), "Evaluating the settlement of lightweight coarse aggregate in self-compacting lightweight concrete", *Comput. Concrete*, **19**(2), 203-210.
- Mazloom, M. and Miri, M.S. (2017), "Interaction of magnetic water, silica fume and superplasticizer on fresh and hardened properties of concrete", *Adv. Concrete Constr.*, **5**(2), 87-99.
- Mazloom, M., Pourhaji, P., Moosa Farash, A. and Sanati A. (2018a), "Strengthening of concrete structures with buckling braces and buckling restrained braces", *Struct. Monit. Maint.*, **5** (3), 391-416.
- Mazloom, M. Ramezaniapour, A.A. and Brooks, J.J. (2004), "Effect of silica fume on mechanical properties of high-strength concrete", *Cement Concrete Compos.*, **26**(1), 347-357.
- Mazloom, M. and Ranjbar, A. (2010), "Relation between the workability and strength of self-compacting concrete", *Proceedings of the 35th Conference on our world in concrete & structure*, Singapore, August.
- Mazloom, M., Saffari A. and Mehrvand, M. (2015), "Compressive, shear and torsional strength of beams made of self-compacting concrete", *Comput. Concrete*, **15**(6), 935-950.
- Mazloom, M, Soltani, A., Karamloo, M., Hassanloo, A. and Ranjbar, A. (2018d), "Effects of silica fume, superplasticizer dosage and type of superplasticizer on the properties of normal and self-compacting concrete", *Adv. Mater. Res.*, **7**(1), 407-434.
- Mazloom, M. and Yoosefi, M.M. (2013), "Predicting the Indirect Tensile Strength of Self Compacting Concrete Using Artificial Neural Networks", *Comput. Concrete*, **12**(3), 285-301.
- Nunes, S., Figueiras, H., Oliveira, P.M., Coutinho, J.S. and Figueiras, J. (2006), "A methodology to assess robustness of SCC mixtures", *Cement Concrete Res.*, **36**(12), 2115- 2122.
- Paultre, P., Khayat, K.H., Cusson, D. and Tremblay, S. (2005), "Structural performance of self-consolidating concrete used in confined concrete column", *ACI Struct. J.*, **102**(4), 560-568.
- Sagan, E., Rasheed, H. and Alkhrdaji, T. (2018), "Evaluation of the seismic performance of reinforced concrete frames strengthened with CFRP fabric and NSM bars", *Compos. Struct.*, **184**, 839-847.
- Sharif, A., Al-Mekhlafi, G. and Al-Osta, M. (2019), "Structural performance of CFRP-strengthened concrete-filled stainless steel tubular short columns", *Eng. Struct.*, **183**, 94-109.
- Shin, M. and LaFave, M.L. (2004), "Reinforced concrete edge beam-column-slab connections subjected to earthquake loading", *Mag. Concrete Res.*, **55**(6), 273-291.
- Silva, M., Biscaia, H. and Marreiros, R. (2013), "Bond-slip on CFRP/GFRP-to-concrete joints subjected to moisture, salt fog and temperature cycles", *Compos. Part B: Eng.*, **55**, 374-385.
- Taqieddin, Z.N. (2008), "Elasto-Plastic and damage modeling of reinforced concrete", Ph.D. dissertation, Louisiana State University, Baton Rouge LA.
- Zhou, L., Zheng, Y. and Taylor, S. (2018), "Finite-element investigation of the structural behavior of basalt fiber reinforced polymer (BFRP)-reinforced self-compacting concrete (SCC) decks slabs in Thompson bridge", *Polymers J.*, **10** (6), 67-702.